BIOCHEMISTRY
including biophysical chemistry & molecular biology
Article

Biochemistry **2009,** *48,* 6085–6094 6085
DOI: 10.1021/bi900003t

Crystal Structure of the Bacterial Luciferase/Flavin Complex Provides Insight into the Function of the β Subunit[†,‡]

Zachary T. Campbell,[§] Andrzej Weichsel,[§] William R. Montfort,[§] and Thomas O. Baldwin*[,§,⊥]

[§]*Department of Biochemistry and Molecular Biophysics, University of Arizona, 1041 East Lowell Street, Biological Sciences West, Tucson, Arizona 85721-0088, and* [⊥]*Department of Biochemistry, University of California, Riverside, California 92521*

Received January 2, 2009; Revised Manuscript Received May 10, 2009

ABSTRACT: Bacterial luciferase from *Vibrio harveyi* is a heterodimer composed of a catalytic α subunit and a homologous but noncatalytic β subunit. Despite decades of enzymological investigation, structural evidence defining the active center has been elusive. We report here the crystal structure of *V. harveyi* luciferase bound to flavin mononucleotide (FMN) at 2.3 Å. The isoalloxazine ring is coordinated by an unusual *cis*-Ala-Ala peptide bond. The reactive sulfhydryl group of Cys106 projects toward position C-4a, the site of flavin oxygenation. This structure also provides the first data specifying the conformations of a mobile loop that is crystallographically disordered in both prior crystal structures [Fisher, A. J., Raushel, F. M., Baldwin, T. O., and Rayment, I. (1995) Biochemistry *34*, 6581−6586; Fisher, A. J., Thompson, T. B., Thoden, J. B., Baldwin, T. O., and Rayment, I. (1996) J. Biol. Chem. 271, 21956−21968]. This loop appears to be a boundary between solvent and the active center. Within this portion of the protein, a single contact was observed between Phe272 of the α subunit, not seen in the previous structures, and Tyr151 of the β subunit. Substitutions at position 151 on the β subunit caused reductions in activity and total quantum yield. Several of these mutants were found to have decreased affinity for reduced flavin mononucleotide ($FMNH_2$). These findings partially address the long-standing question of how the β subunit stabilizes the active conformation of the α subunit, thereby participating in the catalytic mechanism.

Biological light emission has fascinated mankind for centuries. It is now accepted that the diverse molecular mechanisms for light emission have evolved independently multiple times in organisms ranging from bacteria to fungi to insects and teleost fish. Bacterial luciferase is a heterodimeric (αβ) flavin monooxygenase that catalyzes the reaction of $FMNH_2$,[1] O_2, and an aliphatic aldehyde to yield FMN, the corresponding carboxylic acid, and blue-green light (Figure 1 (*1*, *2*)). The reduced flavin substrate is reversibly bound to form a noncovalent complex. *In vivo*, the reduced flavin is bound from solution rather than by transfer from an NAD(P)H-dependent oxidoreductase (*3*). This intermediate reacts with molecular oxygen to form the 4a,5-dihydro-4a-hydroperoxyflavin (intermediate-II (*4*)). Aldehyde binding is proposed to lead to formation of a tetrahedral intermediate that decomposes to yield light, carboxylic acid, and oxidized FMN (*5*). Energy for light production comes primarily from oxidation of the aldehyde to the carboxylic acid (*6*). Production of a photon of blue-green light requires approximately 60−80 kcal/mol (*5*). *A priori*, one would assume that such high-energy intermediates would lead to enzyme modification. However, luciferases appear to have structural mechanisms to avoid reaction with such high-energy intermediates.

Bacterial luciferase is composed of two homologous subunits, designated α and β, both of which assume the TIM $(\beta/\alpha)_8$ barrel fold (*7*, *8*). Although the β subunit is required for activity, the catalytic site has been proposed to reside exclusively on the α subunit (*5*, *9*). The active center of the enzyme is thought to be distant from the subunit interface (*10*, *11*). While there is ample evidence for intersubunit communication (*12*, *13*), no structural mechanism utilizing the mobile loop has been proposed prior to this report. Mutations causing altered enzyme kinetics have been found almost entirely on the α subunit (*5*, *13*). Although a precise location on the enzyme for substrate binding has not been demonstrated, three models for flavin binding have been proposed (*10*, *14*, *15*). The first is based upon the high-resolution crystal structure (*8*). Using computational docking, flavin analog binding, and mutagenesis studies, Lin and co-workers (*10*) positioned the isoalloxazine ring adjacent to the nonprolyl *cis*-peptide bond (*8*). The validity of the computationally derived model was examined in a recent mutagenesis study (*16*). Substitutions were introduced near the proposed isoalloxazine binding site at Ala75 and Cys106. These mutations resulted in spectral red shifts

[†]This research was supported, in part, by NIH Grant HL62969 to W.R.M. Portions of this research were carried out at the Stanford Synchrotron Radiation Laboratory, a national user facility operated by Stanford University on behalf of the U.S. Department of Energy, Office of Basic Energy Sciences.

[‡]Coordinates of the luciferase/FMN complex have been deposited with the Protein Data Bank under the accession number 3FGC.

*To whom correspondence should be addressed. Mailing address: College of Natural and Agricultural Sciences, 900 University Avenue, 302 College Building North, Riverside, CA 92521. Phone: (951) 827-3101. Fax: (951) 827-4190. E-mail address: thomas.baldwin@ucr.edu.

[1]Abbreviations: FMN, flavin mononucleotide; $FMNH_2$, reduced flavin mononucleotide; IPTG, isopropyl-β-D-thiogalactopyranoside; SDS−PAGE, sodium dodecyl sulfate polyacrylamide gel electrophoresis; CD, circular dichroism.

Published on Web 05/12/2009

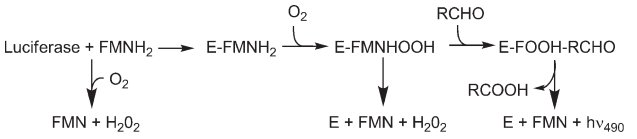

FIGURE 1: The mechanism of bacterial bioluminescence *in vitro*.

up to 10 nm. In the second model of flavin binding, the low-resolution structure was used to guide the placement of FMN based on structural similarity to methylenetetrahydromethanopterin reductase (MER) (*7*, *14*). FMN was modeled into the approximate location of the MER F_{420} cofactor. In the third model, the structure of the β_2 homodimer was used to place the phosphate group of the flavin in a solvent-exposed cleft near the subunit interface (*15*). This model places the isoalloxazine ring in solvent. We report the experimentally determined structure of the luciferase/FMN complex and find that two of the modeled structures (*10*, *14*) are approximately correct and one is not (*15*).

To date, only two mutations have been identified in the β subunit that result in altered substrate affinity in the α subunit, the lesion giving rise to the FB-1 phenotype and several mutants of residue His82 (*12*, *13*, *17*). Luciferase does not appear to undergo subunit exchange under standard conditions *in vitro* (*18*). In an elegant set of complementation experiments, it was found that FB-1 can provide functional α subunit to luciferase variants with defective α subunits (*17*), demonstrating that, at least for FB-1, a mutation in the β subunit can result in reduced $FMNH_2$ binding affinity and reduced subunit affinity. Unfortunately, the location of the genetic lesion giving rise to FB-1 is unknown because the original stock has been lost (J. W. Hastings, personal communication). In the crystal structure that we describe here, there are two heterodimers in the asymmetric unit, one with flavin bound and the other flavin-free. The mobile loop on the α subunit bound to FMN adopts a distinct structure relative to the FMN-free subunit. A hydrophobic contact was observed between the mobile loop at position αPhe272 and Tyr151 on the β subunit. In order to test whether this contact has significance in the catalytic mechanism of luciferase, a series of substitutions were made at this position. We found that mutation of βTyr151 caused the same phenotype as FB-1, except that the heterodimer dissociation constant was not altered.

EXPERIMENTAL PROCEDURES

Protein Purification. *Vibrio harveyi* luciferase was amplified from the pJHD500 (*19*) plasmid using the nucleotide primers 5′-GAGCCCCTCGAGCGAGTGATATTTG and 5′-CCATATGAAATTCGGAAACTTCCTTC (IDT). The resulting insert was prepared in the same manner as before and ligated into a pET21b vector (Novagen). The vector resulted in the addition of a series of six histidine residues onto the C-terminus of the *luxB* gene. Sequencing of the entire insert was used to verify fidelity (ARL sequencing facility, University of Arizona). A single correct clone was designated pZCH2. Protein was expressed from pZCH2 in a BL21 (λDE3) cell line after growth to an OD_{600} of 0.5 (Stratagene). Expression was initiated by the addition of IPTG to 1 mM. Expression continued for ~6.5 h at 25 °C with constant agitation. Clarified lysate was applied to a custom nickel affinity column (Amersham) and purified to >90% purity assessed by SDS−PAGE analysis (*20*). Purified protein was dialyzed extensively into buffer containing 100 mM Na^+/K^+ phosphate and 100 mM NaCl, pH 7.0. Concentrations of luciferase and the individual α and β subunits were determined using extinction coefficients at 280 nm of 1.136, 1.41, and 0.71 $(mg/mL)^{-1}$ cm^{-1} respectively (*9*).

Protein Crystallization. Luciferase was concentrated to 20 mg/mL using a BIOMAX centrifugal filter (Millipore) and crystallized by the hanging drop method. The sample was mixed 1:1 with 5 μL of precipitant solution containing 100 mM Na^+/K^+ phosphate, pH 7.5, and 1.65 M ammonium sulfate resulting in spontaneous crystal formation after three days. The crystals were soaked with FMN (ICN Biomedicals, final concentration 1 mM) for a period of 6 h under dark conditions at room temperature. Crystals were briefly soaked in a solution containing 1 mM FMN, 100 mM Na^+/K^+ phosphate, pH 7.5, and saturated ammonium sulfate prior to flash freezing in liquid nitrogen (*21*). Diffraction data were collected at the SSRL radiation source using a MAR CCD detector. Reflections were processed using HKL2000, DENZO, and SCALEPACK (*22*). Subsequent analysis and refinement was carried out with a combination of CCP4i, and Coot (*23*−*25*). The structure was solved by molecular replacement using the high resolution structure and molrep (*8*, *25*). The asymmetric unit part of the unit cell contains two non-symmetry-related luciferase heterodimers. The electron density for FMN was far better in chain A of heterodimer 1. All cartoon representations were generated with PyMol (*26*). Hydrogen bonding distances shown in Table 3 were determined using Chimera (*27*). FMN was modeled and refined using a modified CCP4i library to include the C7 and C8 methyl groups in the plane of the isoalloxazine ring (*24*).

Kinetic Assays. Specific activity measurements were determined by the flavin injection assay (*28*). Aliquots of enzyme were incubated in 1.0 mL of 100 mM Na^+/K^+ phosphate containing 0.5 mg/mL BSA and 0.001% aldehyde. The reaction was initiated with the rapid injection of 50 μM photoreduced $FMNH_2$. Flavin was photoreduced using white fluorescent light in the presence of EDTA (*18*). Peak luminescence was recorded using a custom benchtop luminometer (*29*). Aldehyde dependence was measured using the flavin injection assay varying the aldehyde incubated with enzyme. The rate of luminescence decay ($\tau = 0.69/t_{1/2}$) was determined from the elapsed time for the light intensity to decay by 50% ($t_{1/2}$). Total quantum yield was determined based on the equation $I(t) = I_0 2^{-t/t_{1/2}}$. The yield was calculated based on integration over the first 100 s of the reaction using the observed values of I_0 and $t_{1/2}$. *In vivo* activity measurements were made on 1.0 mL aliquots. Light emission was recorded following the rapid injection of 1.0 mL of 0.1% decanal (v/v in water). Peak luminescence was reached ~5 s after injection and recorded.

Thermal Inactivation. Thermostability was determined by monitoring loss of activity as a function of time. Samples (1.0 mL) were incubated at 37 °C in 100 mM Na^+/K^+ phosphate, pH 7.0. Aliquots were withdrawn as a function of time and assayed using the standard flavin injection assay as described above (*28*). Data were analyzed based on curve fitting to first-order decomposition.

Analytical Ultracentrifugation. Molecular weights for several variants were determined using sedimentation equilibrium using a Beckman XL-A centrifuge as described with minor modifications (*30*). Samples were adjusted to an absorbance at 280 nm of approximately 0.8. Reference cells containing buffer alone (50 mM Na^+/K^+ phosphate, 0.1% sodium azide, and 200 mM NaCl, pH 7.0) were used for blank measurements prior to each scan. Data were measured from two cells per sample. Equilibrium was achieved after 12 h at 20 °C using three different speeds, 10 000, 12 500, and 15 000 rpm. Data were collected at

280 nm using an average of 25 passes and a 0.001 cm step size. Data were analyzed based on fitting the data to a single sedimenting species (eq 1)

$$C_r = C_0 \exp\{[M(1-\nu\rho)\omega^2/(2RT)](r^2 - r_0^2)\} + E \quad (1)$$

where C is the concentration at either the initial radial position (C_0) or a given radial position (C_r). The average molecular weight (M) is not fixed during data analysis. Initial estimates for this parameter were assigned on the basis of the calculated molecular weight. The partial specific volume (ν) was calculated from the primary sequence using SEDNTERP (http://www.rasmb.bbri.org/) developed by Hayes, Laue, and Philo. Solvent density (ρ) was calculated based on known solvent composition using SEDNTERP. Data were fit under all three experimental conditions using Kaleidagraph software (Synergy). R^2 values and residual distributions were used to estimate the accuracy of each nonlinear least-squares fit.

RESULTS

Structural Characterization of the Luciferase/FMN Complex. Crystals of recombinant luciferase were grown at room temperature prior to soaking with millimolar concentrations of FMN. After several hours of exposure to flavin, crystals developed a yellow color suggestive of flavin binding. We determined the structure of the enzyme−FMN complex to 2.3 Å resolution using molecular replacement based on the high-resolution structure (Table 1) (*8*).

In the asymmetric unit, there are two non-symmetry-related heterodimers, one of which displays interpretable data for FMN (Figure 2a). Overall, the occupancy of the isoalloxazine site was approximately 50% (Figure 2b,c), likely the result of weak binding (K_d > 100 μM in 50 mM phosphate buffer, pH 7.0) (*31*). The strong electron density for the phosphate moiety of the FMN suggests that binding of either sulfate or phosphate from the crystallization buffer may be competitive with FMN, consistent with the experimental observation in solution that binding of phosphate is competitive with binding of FMN (*32*). In the final model, free phosphate was modeled into both subunit A (50% occupancy) and subunit C (70% occupancy), and FMN was modeled into subunit A at 50% occupancy. In contrast to the MER-based model, we observe a largely planar conformation of the isoalloxazine (*14*). The 5′ phosphate binding site comprises the side chains of Arg107, Arg125, Glu175, Ser176, and Thr179 and the backbone amide of Glu175 (Figure 2d). The side chain of Glu175 exists in two conformations, one of which allows for the carboxylate to hydrogen bond with free phosphate. The binding of oxidized flavin appears to disrupt this interaction. Subunit A also displays a slight collapse of the binding site as compared with subunit C, possibly induced by ligand binding.

Alkylation of the reactive thiol at position 106 of the α subunit has been shown to cause inactivation (*33*). Binding of FMN or aldehyde protected the thiol from alkylation, suggesting that the reactive thiol must reside in or near the substrate binding site (*33*). Mutations of this cysteine destabilize intermediate II but do not inactivate the enzyme (*34*). In our structure, we observe the reactive thiol near O2′ (bound to carbon 4 of the isoalloxazine) projecting at C-4a of the isoalloxazine ring (Figure 2d). The reactive thiol is greater than 11 Å from the closest approach of the β subunit, contrary to the report of Paquette et al., which was based on chemical cross-linking (*35*).

Table 1: Crystallography statistics[a]

space group	$P2_12_12_1$
cell dimensions	
a, *b*, *c* (Å)	58.9, 109.3, 301.4
α, β, γ (deg)	90.0, 90.0, 90.0
resolution (Å)	27.3−2.3
R_{sym} or R_{merge}	0.096 (0.429)
$I/(\sigma I)$	43.3 (6.7)
completeness (%)	99.9 (100)
redundancy	11.1 (11.1)
refinement	
resolution (Å)	27.3−2.3
No. reflections	83087
R_{work}/R_{free}	0.184/0.24
no. atoms	11947
protein	10957
ligand/ion	112
water	876
B-factors	
average (Å^2)	26.8
rms deviations	
bond lengths (Å)	0.020
bond angles (deg)	1.68

[a] Values for the highest resolution bin are given parenthetically.

Vervoort and co-workers (*36*) studied luciferase-bound FMN using NMR methods. Hydrogen bonding was determined on the basis of chemical shifts of isotopically labeled FMN. The model for FMN binding described here was reconciled with the available NMR data (Figure 2e). Hydrogen-bond donor and acceptor pairs were suggested on the basis of the NMR data using functional groups close to FMN observed in our model. Based on our structure, position N-1 may act as a weak hydrogen bond acceptor from the C2′ ribitol hydroxyl group. The carbonyl oxygen at position C-2 accepts hydrogen bonds from a water molecule or the backbone amide hydrogen of Tyr110. The nitrogen at position 3 acts as a hydrogen bond donor to a bound water or the backbone carbonyl oxygen of Glu43. The carbonyl oxygen at position C-4 acts as a hydrogen bond acceptor to either the backbone amide proton or the enol form of the backbone carbonyl oxygen of Ala75. Each of these observed contacts is consistent with the interpretations of Vervoot et al. from NMR chemical shifts (*36*). The isoalloxazine ring of the flavin is held in place almost entirely through backbone contacts. Several residues, including Glu175 and Phe6 in the substrate binding cavity assume different conformations upon FMN binding (Figure 2d).

Structural Characterization of the Mobile Loop. In the present structure, we observe electron density for a portion of the α subunit connecting β strand 7 to α helix 7 (Figure 3a) that was not observed previously (*7*, *8*). This region of the protein is highly protease-labile (*37*). Binding of either FMN or polyvalent anions protects the enzyme from proteolytic inactivation (*37*, *38*). This loop, which is the most highly conserved region of the luciferase sequence (Figure 3b), is adjacent to the active center and appears to undergo a conformational change between a proteolytically labile and a protected form of enzyme (*5*). For each heterodimer in the asymmetric unit, we observed a distinct conformation of this loop, but neither conformation had clear electron density for the backbone between residues 283 and 290 (Figure 3a). This small disordered region is adjacent to the flavin binding cavity. The mobile loop of the flavin-free α subunit contains a secondary structural element composed of two antiparallel β strands near

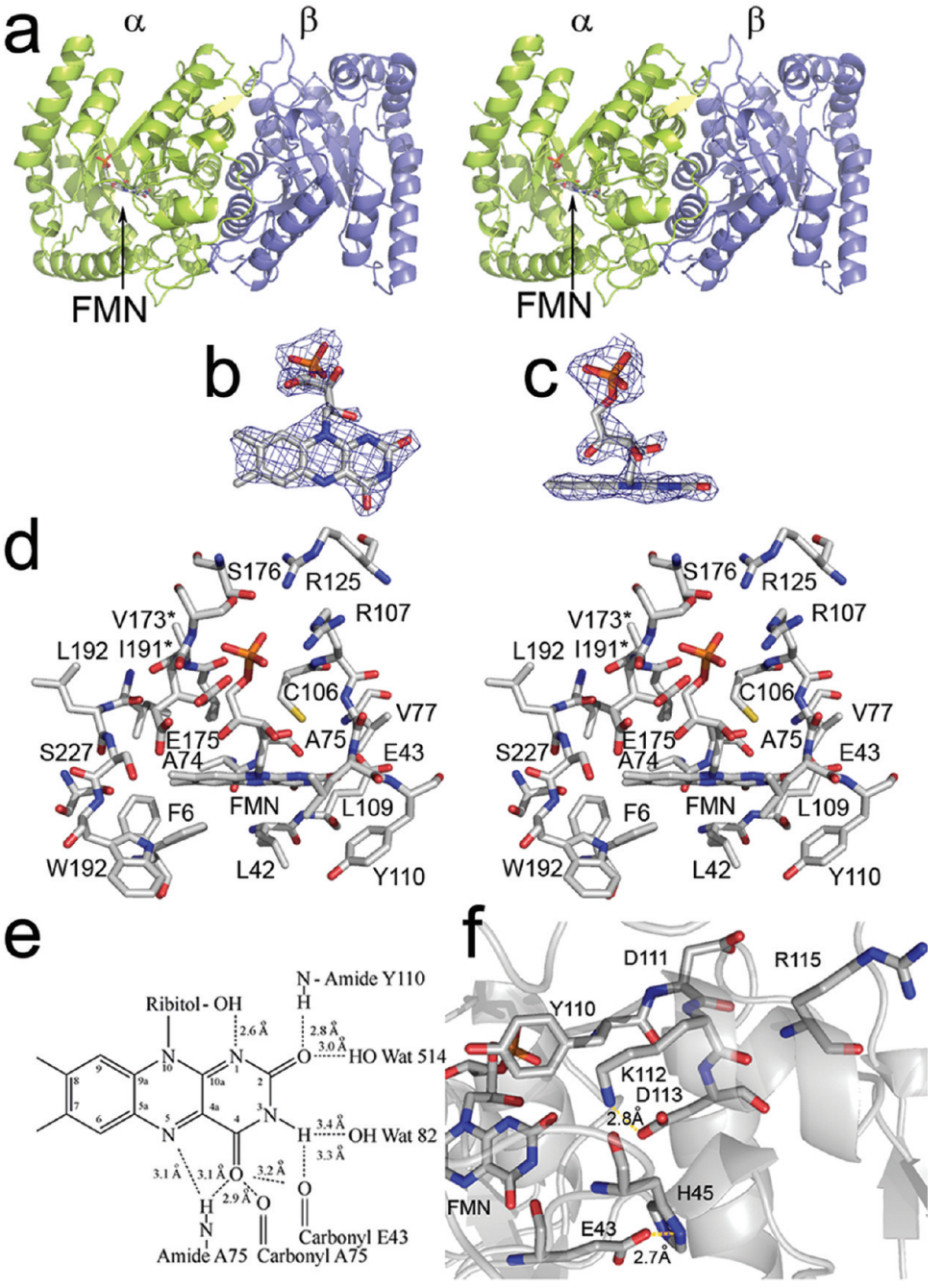

FIGURE 2: (a) Structure of FMN-bound luciferase in stereo. The α subunit is shown in green and the β subunit is shown in purple. The location of the bound FMN is indicated by an arrow. (b) Electron density of the flavin is shown at a contour level of 0.8σ. (c) The same image as in panel b rotated 90°. (d) Residues within 5 Å of the flavin in stereo. Phe6 and Glu175 assume two conformations. The ∗ denotes residues present in the image that are obscured by other atoms. (e) Reconciliation of NMR chemical shifts using isotopically labeled FMN with the observed crystal structure (*36*). Distances were calculated based on heavy atoms. (f) The hydrogen bonding network near the site of AK-6 (*49*, *61*). Both FMN and the charged residues within 5 Å of Asp113 are depicted in the cartoon. The distance between Glu43 and His45 is indicated.

the interface with the β subunit. A single interaction between the mobile loop and the β subunit is formed between α 272 and β 151 (Figure 3c,d).

Biochemical Characterization of βTyr151. It has been clearly demonstrated that the individual subunits of luciferase have low but detectable bioluminescence activity (*9*, *39*). To date, the vast majority of mutants of luciferase that cause significant changes in the kinetic properties of the enzyme have been found to reside in the α subunit (*40*). In order to examine the significance of the contact between the α and β subunits via the mobile loop, a series of substitutions at position Tyr151 were constructed and analyzed. The kinetic pattern of aldehyde chain-length dependence for the mutants at Tyr151 is similar to that of the wild-type enzyme (Table 2). The binding affinities of the Y151K and Y151W mutants for decanal were not significantly different from wild-type (data not shown). These results suggest that the aldehyde binding site is not impacted by these mutations. Virtually all of the mutations led to significant losses in specific activity and total quantum yield. Most of the reported mutations in the β subunit have a minimal impact on activity (*12*). However, substitution of tyrosine β151 with tryptophan, alanine, aspartic acid, and lysine all caused significant losses in activity to levels $< 1\%$ of the wild-type level. Substitutions with arginine, threonine, or valine led to modest losses in activity to 1−11%.

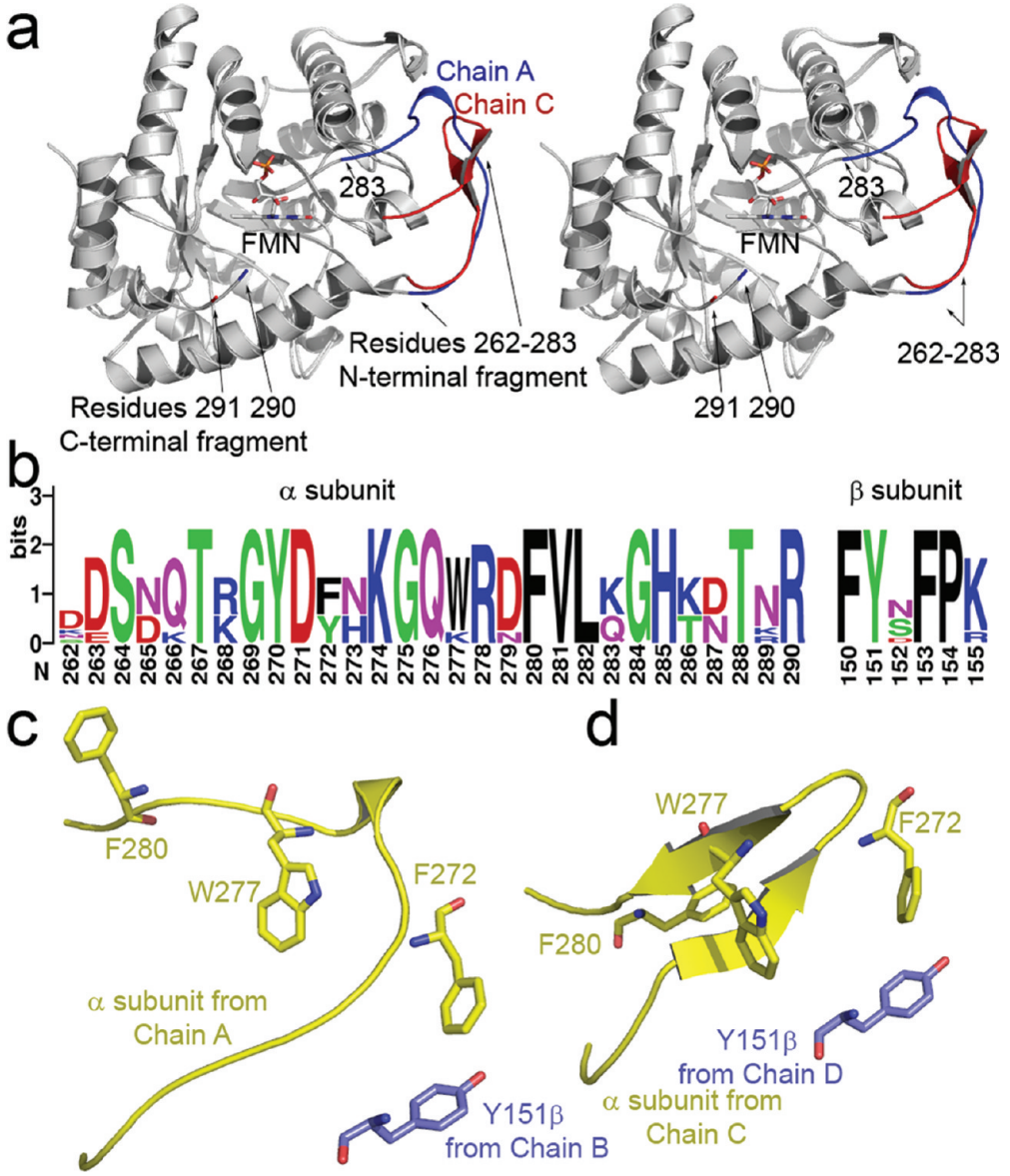

FIGURE 3: (a) Stereoview of the two observed conformations of the mobile loop superimposed upon one another (α262−291). The location of bound FMN is indicated by an arrow. The α subunit observed in a complex with FMN is shown in red. The flavin-free α subunit is shaded in blue, note the location of residues 290 (bound) and 291 (flavin-free); unambiguous electron density for the backbone between residues 284 and 289 was not observed. (b) Multiple sequence alignment of residues in the mobile loop and the hydrophobic segment near βTyr151. Sequences were retrieved from eight species having complete *luxA* and *luxB* entries in the ExPASy database (*62*). Alignment was preformed using ClustalX prior to construction of the sequence logo (*63*, *64*). (c, d) The position of residue 151 on the β (purple) subunit is indicated relative to hydrophobic residues in the mobile loop from the α subunit (yellow). The conformation of the α subunit bound to FMN (c) lacks the pair of antiparallel sheets formed in the flavin-free α subunit (d).

Finally, mutation to phenylalanine or isoleucine had little effect on activity. In order to determine the cause of activity loss, all mutants were tested for the ability to bind $FMNH_2$.

The observed reduction in catalytic efficiency could be the result of a number of different factors. The mobile loop of luciferase is thought to be responsible for protecting reaction intermediates and preventing the entry of bulk solvent into the active center once the flavin substrate is bound (*18*). Deletion of the mobile loop is known to cause weaker binding of $FMNH_2$ (*18*). To determine whether our mutants had reduced $FMNH_2$ binding affinity, we used a method previously described by Cline and Hastings (*13*). Mutant enzymes were assayed using the dithionite method at two concentrations of $FMNH_2$, 2.5 and 25 μM. The difference between these values should be no greater than 20% for wild-type enzyme. We observed a difference of 8% for wild-type protein and greater than 50% for Y151A, Y151D, Y151K, Y151R, and Y151T. These data demonstrated that some mutations at position 151 caused changes in the affinity of luciferase for $FMNH_2$. Therefore, reduced flavin dissociation constants were determined for the most severe of the flavin binding mutants (Figure 4). Using nonlinear regression, we determined the dissociation constant for wild-type enzyme to be 1.1 μM, similar to the values obtained both by Cline and Hastings (*13*) and by Sparks and Baldwin (*18*). The mutant enzymes all bound $FMNH_2$ more weakly. The values are as follows: Y151A, 22.7 μM; Y151K, 17.9 μM; Y151D, 17.6 μM; Y151R, 14 μM; Y151T, 13 μM.

At least two plausible hypotheses predict this difference in flavin binding. Either the active conformation of the mobile loop is no longer being stabilized by the β subunit, or mutation of Tyr151 substantially alters the affinity of the α subunit for the β subunit. In order to exclude the second possibility,

Table 2

	relative specific activity[a]			τ^b			relative quantum yield[c]		
	octanal	decanal	dodecanal	octanal	decanal	dodecanal	octanal	decanal	dodecanal
wt	100	100	100	0.06	0.43	0.05	100	100	100
Y151A	0.027	0.042	0.85	0.10	0.41	0.05	0.02	0.05	0.92
Y151D	0.13	0.40	0.36	0.09	0.50	0.05	0.08	0.41	0.36
Y151F	4.2	9.8	7.2	0.05	0.46	0.05	4.5	14	7.4
Y151I	15	96	31	0.06	0.45	0.04	16	91	35
Y151K	2.3	0.71	0.46	0.10	0.44	0.06	1.3	0.68	0.02
Y151R	10	9.5	22	0.05	0.43	0.06	13	9.5	19
Y151T	1.0	6.5	3.4	0.07	0.43	0.07	0.79	6.5	2.4
Y151 V	13	13	18	0.19	0.50	0.05	3.5	10	17
Y151W	0.006	0.011	0.012	0.07	0.46	0.09	0.005	0.01	0.007

[a] Specific activities of purified protein were determined by the standard $FMNH_2$ injection assay (*28*). Wild-type protein had a specific activity of 5.45×10^{12}, 8.96×10^{13}, and 1.58×10^{11} quanta s^{-1} mg^{-1} using octanal, decanal, or dodecanal, respectively. [b] The decay rate was based on the following calculation $I(t) = I_0 2^{-t/t_{1/2}}$; where $t_{1/2} = \tau \ln 2$. Half-lives were determined based on the time for bioluminescence to decay from the decrease from 80% of the maximum light measurement to 40%. [c] Total quantum yield was determined over the first 100 s of exponential decay. The relative yield was determined by normalizing values for each of the mutants to that of the wild-type enzyme.

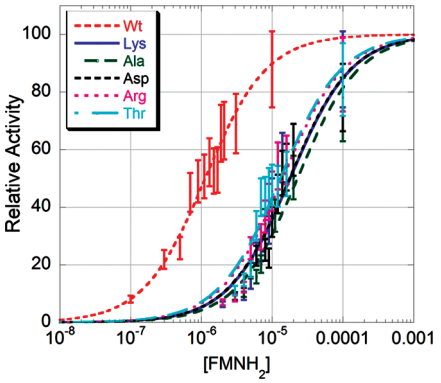

FIGURE 4: Determining the $FMNH_2$ dissociation constant for mutants at position 151β. Initial velocity was determined at different concentrations of substrate and analyzed using the Michaelis–Menten equation (*18*).

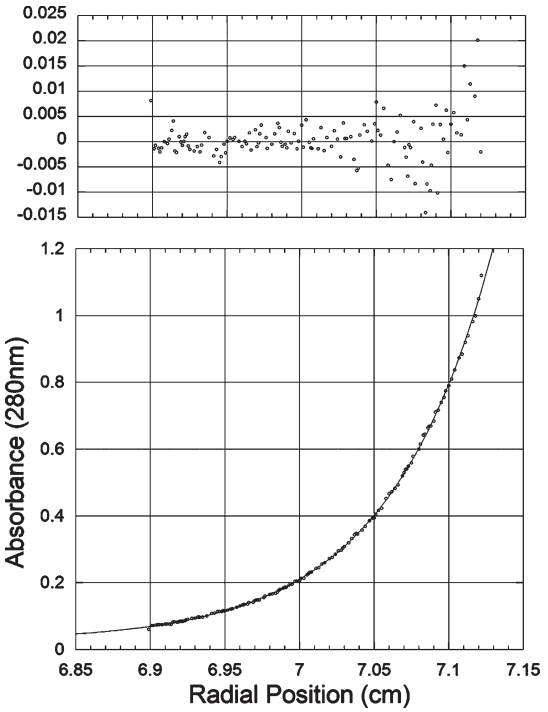

FIGURE 5: Representative sedimentation equilibrium analytical ultracentrifugation data. This sample was centrifuged at 15 000 rpm in 50 mM Na^+/K^+ phosphate, 0.1% sodium azide, and 200 mM NaCl, pH 7.0. Equilibrium was achieved after approximately 12 h at 20 °C. The residuals determined based on nonlinear least-squares curve fitting are shown on the upper panel. All of the samples were fit in a similar manner to a single sedimenting species. The molecular weight for this sample was determined to be 72 953 Da.

sedimentation equilibrium experiments were performed. Wild-type enzyme does not have a detectable subunit dissociation using this technique, which has been estimated to be in the nanomolar range (*18*). The data collected for both the wild-type enzyme and all of the mutants showed a single sedimenting species. The values obtained from least-squares analysis were 77 578 Da for wild-type ($R^2 = 0.9996$, expected MW 77 564 Da), 77 790 Da for Y151W ($R^2 = 0.9976$), 72 953 Da for Y151D ($R^2 = 0.9998$, Figure 5), and 73 938 Da for Y151R ($R^2 = 0.9998$). Each of these values were within 1% of the expected result, consistent with reasonable error of this technique (*41*). Although deletion of the mobile loop is known to cause a detectable dissociation of the heterodimer, mutations of tyrosine 151 on the β subunit do not cause detectable dissociation of the luciferase heterodimer.

The least active mutant (Y151W) appeared to bind reduced flavin with wild-type affinity. In order to investigate the basis of the observed loss in activity, a comparison in thermostability to wild-type enzyme was conducted. Samples were incubated at 37 °C, and aliquots were assayed using the standard $FMNH_2$ injection technique (*28*). Wild-type enzyme had a 90% reduction in activity after 92 min. We found a comparable loss for the Y151W variant after only 11 min, suggesting reduced activation energy for the thermal inactivation reaction.

DISCUSSION

Because $FMNH_2$ is the substrate for the reaction, we attempted to determine the structure of the luciferase/$FMNH_2$ complex using two approaches. In the first, crystals containing FMN were subjected to treatment with sodium dithionite in order to reduce the flavin. These crystals degraded rapidly and were unsuitable for data collection. In the second method, cocrystals were obtained under anaerobic conditions in the presence of dithionite. While these conditions yielded promising visibly colorless orthorhombic crystals, models based upon

diffraction patterns from these crystals were comparable to those obtained under aerobic conditions. It is unclear whether the similarity of the cocrystals was due to oxidation of the flavin during cryprotection or the structures are in fact the same. Additional screening experiments are needed to identify crystallization conditions amenable to the preservation of the enzyme/substrate complex.

In the crystal structure that we describe here, there are two non-symmetry-related α/β heterodimers. The structures of the mobile loop in the two α subunits are different. This result was surprising, given that in both prior crystal structures, this feature was crystallographically disordered (*7*, *8*). In one of the prior structures, the space group was the same as the space group we describe here (*7*). The loop from this structure is disordered over a 15 residue interval between positions 272 and 287 (*7*). We were able to improve upon this structure by resolving the loop region with the exception of 7 residues between positions 283 and 290. This structure was determined after soaking experiments with the product of the reaction, FMN. There was clear electron density in the proposed active center allowing for placement of FMN.

Several models have been proposed for the binding of flavin to luciferase (*10*, *14*, *15*). Our structure is consistent with two of the previous models (*10*, *14*). However, in the third model, the structure of the β_2 homodimer was used to place the 5′ phosphate of the flavin at the subunit interface near αHis82 and βHis82 (*15*). The orientation of the isoalloxazine into solvent, with the ribitol side chain and 5′ phosphate group located at the subunit interface, proposed in this model is inconsistent with the model we obtained of flavin bound to the α subunit. The solvent-filled channel at the β_2 homodimer interface into which Tanner et al. (*15*) modeled the flavin is also present in the $\alpha\beta$ heterodimer (*7*, *8*). Yet, there is no evidence in our data to suggest flavin binding to the site proposed by Tanner et al.

Bacterial luciferase is known to bind tightly to polyvalent anions, such as phosphate (*37*, *42*, *43*). Binding substrate or phosphate stimulates a conformational change in the mobile loop region (*38*). In the low-resolution crystal structure, a phosphate molecule is bound in the same location as the 5′ phosphate group of FMN reported here (*7*). Tu and co-workers examined the significance of the coordination of the phosphate group by Arg107 (*43*). Using mutagenesis, the function of this position was determined to be stabilization of the mobile loop region against proteolytic inactivation (*43*). However, this finding does not exclude the existence of alternate phosphate binding sites on the protein. Widespread conformational changes triggered by phosphate binding have been investigated on luciferase from *V. harveyi*, *Photobacterium phosphoreum*, and *V. fischeri* using far UV CD spectroscopy (*44*). Based on CD spectra of luciferase buffered in either 0.01 or 0.33 M phosphate buffer at neutral pH, the single statistically significant structural alteration was observed in *V. harveyi* luciferase. Although the helical and unstructured or turn regions were invariant, the overall β strand content of the enzyme increased by 30% ± 19.5% (*44*). This result suggests that the proteolytically insensitive conformation induced by substrate or phosphate binding contains either longer stretches of β strands or novel β strands. The only apparent increase in β stand content we report in the structure of the luciferase/FMN complex is in the mobile loop conformation from heterodimer 2, chain C. Since flavin binding is predominantly to heterodimer 2, this would appear to be a discrepancy. However, the structural models described here were obtained by soaking and not cocrystallization. Also, the solution CD data were of luciferase in the presence of phosphate, not FMN. Additional experiments are needed to clarify the relationship between the solution data and crystallographic models.

The flavin binding pocket of bacterial luciferase is a large open cavity that is accessible to solvent via an opening located at the C-terminal ends of the β strands of the TIM-barrel structure. One wall of the cavity, distal to the subunit interface, is lined predominantly with hydrophobic residues, while the other side, more proximal to the interface with the β subunit, is lined with charged polar residues, several of which appear to be engaged in salt linkages across the subunit interface (*30*). The orientation of the isoalloxazine ring within the cavity is with the benzenoid portion toward the hydrophobic surface and the quininoid portion proximal to the charged-polar surface. The 8-methyl substituent, located on the benzenoid portion of the isoalloxazine, is oriented toward the outside of the protein and solvent, as predicted by Massey and colleagues based on spectroscopic analysis of luciferase-bound 8-mercapto FMN (*45*−*47*). The ribitol portion of the flavin extends away from the isoalloxazine at ca. 45° above the plane of the *re*-face, allowing the 5′ phosphate to interact with Arg107 and Arg125, near the surface of the protein. This location of the anion binding site is consistent with the kinetic experiments of Tu and colleagues in addition to the model produced by Meighen and colleagues (*10*, *43*).

The ability to easily monitor kinetic defects using simple techniques, such as screening for impaired light production, have allowed for detailed mutagenesis investigations (*5*, *40*). The best characterized mutant with regard to binding of flavin is known as AK-6 (*13*). This mutant binds the aldehyde substrate normally, but the affinity for the flavin substrate is substantially reduced, and the bioluminescence emission spectrum is red-shifted approximately 12 nm (*48*). Cline and Hastings reported a dramatic shift in the pH−activity profile, with a remarkable stability of the 4a-peroxydihydroflavin intermediate at pH 7 and above. Chlumsky determined that the mutation of AK-6 was αD113N (*5*, *49*). In the structure that we determined of luciferase bound to FMN, Asp113 forms a range of electrostatic interactions with αHis44, αLys112, and αHis45 at distances of 5.9, 2.8, and 4.4 Å, respectively (Figure 2f, Table 3). It has been noted that mutation of conserved phenylalanine residues flanking His44 and His45 can result in a substantial reduction in the total quantum yield of bioluminescence and a diminished yield of intermediate-II (*50*). The distance from the Asp113 Oδ2 to the N3 position of the isoalloxazine was 5.9 Å. Based on these distances, even subtle alterations of this multiresidue electrostatic network near the quininoid portion of the isoalloxazine would be expected to be remarkably detrimental to enzymatic function.

Another mutant studied by Cline and Hastings is AK-20, which was reported to have normal flavin binding but dramatically reduced affinity for the aldehyde substrate (*40*). In addition, the aldehyde chain length dependence of AK-20 relative to wild-type enzyme is dramatically altered. In the structure that we determined, the serine Oδ was 3.9 Å away from the 7-methyl group of the isoalloxazine. Ser227 resides in an extremely hydrophobic portion of the active center cavity. It is conceivable that the abundance of tryptophan and phenylalanine residues in the vicinity of the benzenoid portion of the isoalloxazine ring provide an appropriate surface for binding of the aliphatic substrate. Additional data are needed to test this hypothesis.

The aldehyde binding affinity and kinetic chain-length dependence of the mutations at βTyr151 were unaltered relative to wild-type. Likewise, AK-6 and other mutations at α113 have

Table 3: Hypothetical Hydrogen Bonds Involving Position 113 or FMN[a]

donor			acceptor			distance
Hydrogen Bonds Involving Asp113						
Lys	112	NZ	Asp	113	OD1	2.8
Phe	117	N	Asp	113	O	2.9
Asp	113	N	Tyr	110	O	3.1
D−H···FMN						
Thr	179	OG1	FMN	326	O2P	2.3
Glu	175	N	FMN	326	O3P	2.3
Ser	176	N	FMN	326	O3P	2.7
Leu	109	N	FMN	326	O2	2.8
Arg	107	NH2	FMN	326	O1P	3.0
Arg	107	NE	FMN	326	O2P	3.0
Ala	75	N	FMN	326	O4	3.1
Glu	43	N	FMN	326	O4	3.1
Cys	106	SG	FMN	326	O2′	3.3
FMN−H···A						
FMN	326	N5	Ala	74	O	3.2
FMN	326	N3	Glu	43	O	3.3

[a] Hydrogen bonding distances were determined using Chimera (*27*). Interactions within the ligand as well as those involving solvent are not shown. Any potential interactions beyond 3.3 Å are not reported. All distances are given in angstroms.

normal aldehyde binding properties (*49*). These results suggest that the portion of the flavin binding pocket around the quininoidal portion of the isoalloxazine is not associated with aldehyde binding. This interpretation is consistent with the observation that the hydrophobic pocket near the site of the AK-20 lesion is associated with aldehyde binding (*51*).

The folding and assembly of bacterial luciferase subunits have been studied extensively *in vitro* using both refolding and cotranslational folding approaches (*9*, *39*, *52*−*55*). Luciferase forms the active heterodimeric species when diluted from denaturant in a highly concentration-dependent manner (*54*). Both folding and unfolding of the heterodimer occur by a three-state mechanism containing a highly populated but inactive heterodimeric intermediate (*56*). Although the β subunit is capable of forming a homodimeric native state equivalent in stability to that of the heterodimer, the heterodimer is believed to be the predominant product of the *lux*A and *lux*B genes inside of the cell as its formation is kinetically preferred (*30*, *57*, *58*). The individual α and β subunits display bioluminescence activity, but the specific activity is between 10^4 and 10^5 lower than that of the heterodimer (*39*). Because of the enormous difference in activity between the heterodimer and the α subunit alone, it is generally felt that the β subunit stabilizes the active form of the α subunit (*18*, *30*). This hypothesis appears to be entirely consistent with the structure of the luciferase/FMN complex. The quininoid edge of the flavin is within ca. 10 Å of the β subunit, and Asp113, the site of the AK-6 mutation, is ca. 7 Å from β. The central region of the luciferase subunit interface consists of an interesting region of high polarity (*8*, *30*). The present results demonstrate that the FMN binding site inside the α subunit is adjacent to this clustering of charged-polar residues (Figure 2d,f).

Our examination of the FMN/luciferase crystal structure revealed a specific contact between the subunits involving a residue within the mobile loop. We devised a series of experiments based on this observation to determine whether the active conformation of the α subunit is stabilized by the β subunit in part via the mobile loop. We found that a wide variety of mutations at this position, ranging from conservative alanine substitution to nonconservative substitution with aspartic acid, led to comparable losses in activity. The observed defect in generating bioluminescence was unrelated to subunit association. Therefore, it appears likely that one component of the mechanism employed by the β subunit to promote the active conformation of the α subunit involves the preservation of this contact.

Mutations at position βTyr151 were found to have a severe effect on binding of $FMNH_2$ (Figure 4). The least active mutant, Y151W, was apparently the result, at least in part, of destabilizing the protein. For the remaining mutants, it was important to confirm that the mutations had not destabilized formation of the heterodimer. Based on sedimentation equilibrium data, none of the mutants examined caused a detectable increase in the dissociation constant of the heterodimer. It is therefore unlikely that any of these mutants are identical to FB-1 (*13*). Mutations at position β151 appear to inhibit the ability of the FMN-bound conformation of the mobile loop to form. However, additional experiments probing the dynamics of this region are needed.

It is interesting to note that deletion of the mobile loop had minimal impact on binding of $FMNH_2$ relative to the effect of some of the mutations at position 151 on the β subunit (*18*). It is known that after flavin binding, structural rearrangements are required prior to the reaction of oxygen and subsequent formation of intermediate II (*59*). This rearrangement is a slow millisecond event that may involve transitioning of the mobile loop between an open or semiopen state and a closed or bound conformation. Such a large displacement would be consistent with the observed millisecond time scale. If the series of mutations that we described here alter the kinetics or thermodynamics of this structural transition, then the inability to assume the bound conformation may have an inhibitory effect on substrate binding. In a prior study, it was found that substitution of any of three conserved mobile loop residues, Gly284, Gly275, and Phe261, resulted in substantial losses of bioluminescent activity (*60*). It remains unknown how these mutations resulted in distortions of the structural rearrangement of the mobile loop upon anion binding.

In summary, since the structure of bacterial luciferase was determined, several key features of the enzyme have remained elusive (*7*, *8*). Prior to this report, structural evidence linking a specific binding site on the enzyme to any of the reactants or products had not been described. Likewise, precise structural features of a highly conserved mobile loop adjacent to the active center were unknown. The location of the active center based on the structural evidence outlined here is consistent with previous mutagenesis and chemical modification studies (*5*). The electron density of the portion of the mobile loop distal to the flavin binding site suggests that it is not disordered but can adopt several discrete conformations inside of the crystal. Based on the novel conformations of the mobile loop, a mechanism utilized by the β subunit to stabilize the active form of the α subunit has been suggested. Investigations into the dynamics of this region have yet to be described. Although we are now able to begin the process of defining the structural basis of bacterial light emission, the three-dimensional structure of the luciferase/$FMNH_2$ complex, and more to the point, the excited state flavin/luciferase complex, remain to be determined.

REFERENCES

1. Gibson, Q. H., and Hastings, J. W. (1962) The oxidation of reduced flavin mononucleotide by molecular oxygen. *Biochem. J. 83*, 368–377.
2. Hastings, J. W., and Gibson, Q. H. (1963) Intermediates in the bioluminescent oxidation of reduced flavin mononucleotide. *J. Biol. Chem. 238*, 2537–2554.
3. Campbell, Z. T., and Baldwin, T. O. (2009) Fre is the major flavin reductase supporting bioluminescence from *Vibrio harveyi* luciferase in *Escherichia coli*. *J. Biol. Chem. 284*, 8322–8328.
4. Hastings, J. W., Balny, C., Peuch, C. L., and Douzou, P. (1973) Spectral properties of an oxygenated luciferase-flavin intermediate isolated by low-temperature chromatography. *Proc. Natl. Acad. Sci. U.S.A. 70*, 3468–3472.
5. Baldwin, T. O., and Ziegler, M. M. (1992) in Chemistry and Biochemistry of Flavoenzymes (Muller, F., Ed.), pp 467−530, CRC Press, Boca Raton, FL.
6. Hastings, J. W., Eberhard, A., Baldwin, T. O., Nicoli, M. Z., Cline, T. W., and Nealson, K. H. (1973) Bacterial bioluminescence: Mechanistic implications of active center chemistry of luciferase, in Bioluminescence and Chemiluminescence (Cormier, M. J., Hercules, D. M., and Lee, J., Eds.), pp 369−380, Plenum Publishing Co., New York.
7. Fisher, A. J., Raushel, F. M., Baldwin, T. O., and Rayment, I. (1995) Three-dimensional structure of bacterial luciferase from *Vibrio harveyi* at 2.4 Å resolution. *Biochemistry 34*, 6581–6586.
8. Fisher, A. J., Thompson, T. B., Thoden, J. B., Baldwin, T. O., and Rayment, I. (1996) The 1.5-Å resolution crystal structure of bacterial luciferase in low salt conditions. *J. Biol. Chem. 271*, 21956–21968.
9. Sinclair, J. F., Waddle, J. J., Waddill, E. F., and Baldwin, T. O. (1993) Purified native subunits of bacterial luciferase are active in the bioluminescence reaction but fail to assemble into the alpha beta structure. *Biochemistry 32*, 5036–5044.
10. Lin, L. Y., Sulea, T., Szittner, R., Vassilyev, V., Purisima, E. O., and Meighen, E. A. (2001) Modeling of the bacterial luciferase-flavin mononucleotide complex combining flexible docking with structure-activity data. *Protein Sci. 10*, 1563–1571.
11. Baldwin, T. O., Christopher, J. A., Raushel, F. M., Sinclair, J. F., Ziegler, M. M., Fisher, A. J., and Rayment, I. (1995) Structure of bacterial luciferase. *Curr. Opin. Struct. Biol. 5*, 798–809.
12. Xin, X., Xi, L., and Tu, S. C. (1994) Probing the *Vibrio harveyi* luciferase beta subunit functionality and the intersubunit domain by site-directed mutagenesis. *Biochemistry 33*, 12194–12201.
13. Cline, T. W., and Hastings, J. W. (1972) Mutationally altered bacterial luciferase. Implications for subunit functions. *Biochemistry 11*, 3359–3370.
14. Aufhammer, S. W., Warkentin, E., Ermler, U., Hagemeier, C. H., Thauer, R. K., and Shima, S. (2005) Crystal structure of methylenetetrahydromethanopterin reductase (Mer) in complex with coenzyme F420: Architecture of the F420/FMN binding site of enzymes within the nonprolyl cis-peptide containing bacterial luciferase family. *Protein Sci. 14*, 1840–1849.
15. Tanner, J. J., Miller, M. D., Wilson, K. S., Tu, S. C., and Krause, K. L. (1997) Structure of bacterial luciferase beta 2 homodimer: Implications for flavin binding. *Biochemistry 36*, 665–672.
16. Lin, L. Y. C., Sulea, T., Szittner, R., Kor, C., Purisima, E. O., and Meighen, E. A. (2002) Implications of the reactive thiol and the proximal non-proline *cis*-peptide bond in the structure and function of *Vibrio harveyi* luciferase. *Biochemistry 41*, 9938–9945.
17. Anderson, C., Tu, S. C., and Hastings, J. W. (1980) Subunit exchange between and specific activities of mutant bacterial luciferases. *Biochem. Biophys. Res. Commun. 95*, 1180–1186.
18. Sparks, J. M., and Baldwin, T. O. (2001) Functional implications of the unstructured loop in the $(\beta/\alpha)_8$ barrel structure of the bacterial luciferase α subunit. *Biochemistry 40*, 15436–15443.
19. Devine, J. H., Shadel, G. S., and Baldwin, T. O. (1989) Identification of the operator of the lux regulon from the *Vibrio fischeri* strain ATCC7744. *Proc. Natl. Acad. Sci. U.S.A. 86*, 5688–5692.
20. Schagger, H., and von Jagow, G. (1987) Tricine-sodium dodecyl sulfate-polyacrylamide gel electrophoresis for the separation of proteins in the range from 1 to 100 kDa. *Anal. Biochem. 166*, 368–379.
21. Rodgers, D. W. (1994) Cryocrystallography. *Structure 2*, 1135–1140.
22. Otwinowski, Z., and Minor, W. (1997) Processing of X-ray diffraction data collected in the oscillation mode, in Methods in Enzymology (Carter, C. W., and Sweet, R. M., Eds.), pp 307−326, Academic Press, New York.
23. Emsley, P., and Cowtan, K. (2004) Coot: Model-building tools for molecular graphics. *Acta Crystallogr. D60*, 2126–2132.
24. Potterton, L., McNicholas, S., Krissinel, E., Gruber, J., Cowtan, K., Emsley, P., Murshudov, G. N., Cohen, S., Perrakis, A., and Noble, M. (2004) Developments in the CCP4 molecular-graphics project. *Acta Crystallogr. D60*, 2288–2294.
25. Collaborative Computing Project (1994) The CCP4 suite: programs for protein crystallography. *Acta Crystallogr. D50*, 760–763.
26. DeLano, W. L. (2002) The PyMOL Molecular Graphics System, DeLano Scientific.
27. Pettersen, E. F., Goddard, T. D., Huang, C. C., Couch, G. S., Greenblatt, D. M., Meng, E. C., and Ferrin, T. E. (2004) UCSF Chimera–a visualization system for exploratory research and analysis. *J. Comput. Chem. 25*, 1605–1612.
28. Hastings, J. W., Baldwin, T. O., Nicoli, M. Z. (1978) Bacterial luciferase: Assay, purification, and properties, in Methods in Enzymology (DeLuca, M., Ed.), pp 135−152, Academic Press, New York.
29. Mitchell, G. W., and Hastings, J. W. (1971) A stable, inexpensive, solid-state photomultiplier photometer. *Anal. Biochem. 39*, 243–250.
30. Inlow, J. K., and Baldwin, T. O. (2002) Mutational analysis of the subunit interface of *Vibrio harveyi* bacterial luciferase. *Biochemistry 41*, 3906–3915.
31. Baldwin, T. O., Nicoli, M. Z., Becvar, J. E., and Hastings, J. W. (1975) Bacterial luciferase. Binding of oxidized flavin mononucleotide. *J. Biol. Chem. 250*, 2763–2768.
32. Meighen, E. A., and MacKenzie, R. E. (1973) Flavine specificity of enzyme−substrate intermediates in the bacterial bioluminescent reaction. Structural requirements of the flavine side chain. *Biochemistry 12*, 1482–1491.
33. Nicoli, M. Z., Meighen, E. A., and Hastings, J. W. (1974) Bacterial luciferase. Chemistry of the reactive sulfhydryl. *J. Biol. Chem. 249*, 2385–2392.
34. Abu-Soud, H. M., Clark, A. C., Francisco, W. A., Baldwin, T. O., and Raushel, F. M. (1993) Kinetic destabilization of the hydroperoxy flavin intermediate by site-directed modification of the reactive thiol in bacterial luciferase. *J. Biol. Chem. 268*, 7699–7706.
35. Paquatte, O., Fried, A., and Tu, S. C. (1988) Delineation of bacterial luciferase aldehyde site by bifunctional labeling reagents. *Arch. Biochem. Biophys. 264*, 392–399.
36. Vervoort, J., Muller, F., O'Kane, D. J., Lee, J., and Bacher, A. (1986) Bacterial luciferase: A carbon-13, nitrogen-15, and phosphorus-31 nuclear magnetic resonance investigation. *Biochemistry 25*, 8067–8075.
37. Holzman, T. F., and Baldwin, T. O. (1980) Proteolytic inactivation of luciferases from three species of luminous marine bacteria, *Beneckea harveyi*, *Photobacterium fischeri*, and *Photobacterium phosphoreum*: Evidence of a conserved structural feature. *Proc. Natl. Acad. Sci. U.S.A. 77*, 6363–6367.
38. Holzman, T. F., and Baldwin, T. O. (1980) The effects of phosphate on the structure and stability of the luciferases from *Beneckea harveyi*, *Photobacterium fischeri*, and *Photobacterium phosphoreum*. *Biochem. Biophys. Res. Commun. 94*, 1199–1206.
39. Waddle, J., and Baldwin, T. O. (1991) Individual alpha and beta subunits of bacterial luciferase exhibit bioluminescence activity. *Biochem. Biophys. Res. Commun. 178*, 1188–1193.
40. Cline, T. W. (1973) Mutational Alteration of the Bacterial Bioluminescence System. Ph.D. Thesis, Department of Biochemistry and Molecular Biology, Harvard, Cambridge, MA.
41. MacGregor, I. K., Anderson, A. L., and Laue, T. M. (2004) Fluorescence detection for the XLI analytical ultracentrifuge. *Biophys. Chem. 108*, 165–185.
42. Baldwin, T. O., and Riley, P. L. (1980) Anion binding to bacterial luciferase: Evidence for binding associated changes in enzyme structure, in Flavins and Flavoproteins (Yagi, K., and Yamano, T., Eds.), pp 139−147, Japan Scientific Societies Press and University Park Press, Baltimore, MD.
43. Moore, C., Lei, B., and Tu, S. C. (1999) Relationship between the conserved alpha subunit arginine 107 and effects of phosphate on the activity and stability of *Vibrio harveyi* luciferase. *Arch. Biochem. Biophys. 370*, 45–50.
44. Holzman, T. F. (1983) Bacterial Luciferase: Studies of Proteolytic Inactivation and Ligand Binding. Ph.D. Thesis, Department of Biochemistry, University of Illinois, Champaign−Urbana.
45. Murthy, Y. V., and Massey, V. (1998) Synthesis and properties of 8-CN-flavin nucleotide analogs and studies with flavoproteins. *J. Biol. Chem. 273*, 8975–8982.
46. Schopfer, L. M., Massey, V., and Claiborne, A. (1981) Active site probes of flavoproteins. Determination of the solvent accessibility of the flavin position 8 for a series of flavoproteins. *J. Biol. Chem. 256*, 7329–7337.
47. Francisco, W. A., Abu-Soud, H. M., Topgi, R., Baldwin, T. O., and Raushel, F. M. (1996) Interaction of bacterial luciferase with 8-substituted flavin mononucleotide derivatives. *J. Biol. Chem. 271*, 104–110.

48. Cline, T. W., and Hastings, J. W. (1974) Mutated luciferases with altered bioluminescence emission spectra. *J. Biol. Chem. 249*, 4668–4669.
49. Chlumsky, J. L. (1991) Ph.D. Thesis, Department of Biochemistry and Biophysics, Texas A & M, College Station, TX.
50. Li, C. H., and Tu, S. C. (2005) Active site hydrophobicity is critical to the bioluminescence activity of *Vibrio harveyi* luciferase. *Biochemistry 44*, 12970–12977.
51. Chen, L. H., and Baldwin, T. O. (1989) Random and site-directed mutagenesis of bacterial luciferase: Investigation of the aldehyde binding site. *Biochemistry 28*, 2684–2689.
52. Fedorov, A. N., and Baldwin, T. O. (1995) Contribution of cotranslational folding to the rate of formation of native protein structure. *Proc. Natl. Acad. Sci. U.S.A. 92*, 1227–1231.
53. Waddle, J. J., Johnston, T. C., and Baldwin, T. O. (1987) Polypeptide folding and dimerization in bacterial luciferase occur by a concerted mechanism in vivo. *Biochemistry 26*, 4917–4921.
54. Ziegler, M. M., Goldberg, M. E., Chaffotte, A. F., and Baldwin, T. O. (1993) Refolding of luciferase subunits from urea and assembly of the active heterodimer. Evidence for folding intermediates that precede and follow the dimerization step on the pathway to the active form of the enzyme. *J. Biol. Chem. 268*, 10760–10765.
55. Fedorov, A. N., and Baldwin, T. O. (1999) Process of biosynthetic protein folding determines the rapid formation of native structure. *J. Mol. Biol. 294*, 579–586.
56. Clark, A. C., Raso, S. W., Sinclair, J. F., Ziegler, M. M., Chaffotte, A. F., and Baldwin, T. O. (1997) Kinetic mechanism of luciferase subunit folding and assembly. *Biochemistry 36*, 1891–1899.
57. Sinclair, J. F., Ziegler, M. M., and Baldwin, T. O. (1994) Kinetic partitioning during protein folding yields multiple native states. *Nat. Struct. Biol. 1*, 320–326.
58. Thoden, J. B., Holden, H. M., Fisher, A. J., Sinclair, J. F., Wesenberg, G., Baldwin, T. O., and Rayment, I. (1997) Structure of the beta 2 homodimer of bacterial luciferase from *Vibrio harveyi*: X-ray analysis of a kinetic protein folding trap. *Protein Sci. 6*, 13–23.
59. Francisco, W. A., Abu-Soud, H. M., DelMonte, A. J., Singleton, D. A., Baldwin, T. O., and Raushel, F. M. (1998) Deuterium kinetic isotope effects and the mechanism of the bacterial luciferase reaction. *Biochemistry 37*, 2596–2606.
60. Low, J. C., and Tu, S. C. (2002) Functional roles of conserved residues in the unstructured loop of *Vibrio harveyi* bacterial luciferase. *Biochemistry 41*, 1724–1731.
61. Chen, L. H. (1989) Site-Specific Mutagenesis of Bacterial Luciferase. Ph.D. Thesis, Department of Biochemistry and Biophysics, Texas A & M, College Station, TX.
62. Gasteiger, E., Gattiker, A., Hoogland, C., Ivanyi, I., Appel, R. D., and Bairoch, A. (2003) ExPASy: The proteomics server for in-depth protein knowledge and analysis. *Nucleic Acids Res. 31*, 3784–3788.
63. Chenna, R., Sugawara, H., Koike, T., Lopez, R., Gibson, T. J., Higgins, D. G., and Thompson, J. D. (2003) Multiple sequence alignment with the Clustal series of programs. *Nucleic Acids Res. 31*, 3497–3500.
64. Crooks, G. E., Hon, G., Chandonia, J. M., and Brenner, S. E. (2004) WebLogo: A sequence logo generator. *Genome Res. 14*, 1188–1190.